JOURNAL OF CATALYSIS 96, 468–480 (1985)

The Formation of Filamentous Carbon on Iron and Nickel Catalysts

II. Mechanism

A. J. H. M. KOCK, P. K. DE BOKX, E. BOELLAARD, W. KLOP, AND J. W. GEUS

Department of Inorganic Chemistry, State University of Utrecht, Croesestraat 77A, 3522 AD Utrecht, The Netherlands

Received May 31, 1984; revised February 18, 1985

The mechanism of filamentous carbon growth on iron and nickel catalysts has been studied using a combination of magnetic techniques and temperature-programmed hydrogenation. CO and CH_4 were used as carburizing agents. It is concluded that high carbide contents are a prerequisite for the nucleation of filamentous carbon. The presence of a substoichiometric nickel carbide during steady-state growth is established. In the case of iron the hexagonal ε-Fe_2C or ε'-$Fe_{2.2}C$ is proposed to be the intermediate in filamentous growth. The driving force for carbon transport can be appreciated considering the presence of a gradient in the carbon content of nonstoichiometric carbides. © 1985 Academic Press, Inc.

INTRODUCTION

In Part I (*1*) we presented evidence for the involvement of carbide intermediates in filamentous carbon growth on iron and nickel catalysts. The characterization of these carbides under growth conditions as well as the mechanism leading to filament growth is the subject of the present study.

A number of mechanisms explaining filamentous carbon growth on transition metals has been suggested (*2–4*). Carbon can be transported by a surface diffusion process or by bulk diffusion through the particle. Massaro and Petersen (*5*) showed that surface diffusion of carbon on nickel foils is negligibly small in the temperature range 620–970 K. Also the sparse data for surface migration of hydrocarbon species indicate that carbon transport does not proceed through surface diffusion of hydrocarbon fragments (*6*). At present a growth model involving bulk diffusion through the metal particle is generally accepted (*7*). The driving force responsible for this bulk diffusion, however, has not been unequivocally established.

Baker *et al.* (*2, 8*) stated that a temperature gradient across the metal particle due to an exothermic surface reaction was the driving force for whisker growth. In this model carbon segregated at the cold rear of the particle, where the solubility of carbon is smaller. A severe criticism of this model is found in the occurrence of filamentous growth during endothermic decomposition reactions. Baker *et al.* (*9*) have replied that saturated hydrocarbons are known to decompose via their dehydrogenated analogs. Decomposition of the latter compounds is exothermic and, consequently, a mechanism involving thermal diffusion would not be contravened. This explanation, however, calls for separate sites where only the endothermic dehydrogenation takes place.

Rostrup-Nielsen and Trimm (*3*), referring to Wada *et al.* (*10*), assumed that carbon species of different origin have a different solubility. Thus, carbon species at the metal–gas interface originating from hydrocarbon decomposition reactions have a higher solubility than carbon originating from graphite. The resulting concentration gradient is thought to be responsible for carbon transport. However, the physical basis for these different solubilities has not been clarified.

Buyanov *et al.* (*4, 11, 12*) proposed a

0021-9517/85 $3.00
Copyright © 1985 by Academic Press, Inc.
All rights of reproduction in any form reserved.

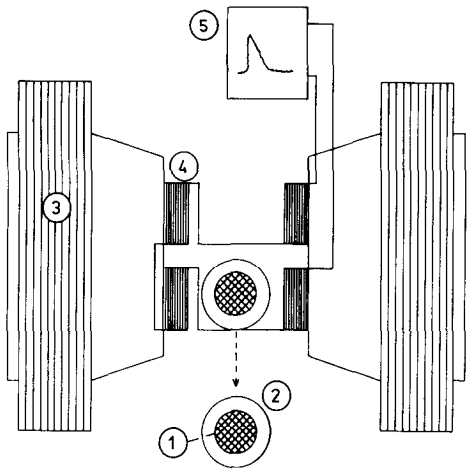

FIG. 1. Schematic diagram of apparatus for magnetic measurements: (1) sample holder, (2) cooler/heater, (3) transportable electromagnet, (4) Helmholtz sensing coils, (5) integrating device.

carbide-cycle mechanism: this invoked consecutive formation and decomposition of carbides, where carbon separated in the latter step leads to the formation of filaments. Thus, no longer interstitial carbon with an extremely low (extrapolated) solubility was considered, but the carbon was supposed to have a carbidic nature.

Previously (*1*), we observed that during carbon whisker growth on iron and nickel catalysts equilibria with carbides were attained. Independently, we established the presence of carbon at concentrations greatly exceeding the solubility of interstitial carbon in iron as well as in nickel, in agreement with prior reports (*13*). Recently, for iron catalysts cementite (θ-Fe_3C) was proposed to be the catalyst for carbon deposition (Sacco *et al.* (*14*)). Baker *et al.* (*9*) observed no carbon whisker growth starting from θ-Fe_3C at all, however. The presence of Eckstrom-Adcock carbide (Fe_7C_3) at the tip of carbon filaments has been demonstrated (*15*).

In this study we present experiments which allow a discrimination to be made between the mechanisms mentioned above. It is very unlikely that a carbon content approximating that of a carbide is attained, when the transport of carbon proceeds through interstitially dissolved carbon. Magnetic measurements enabled us to assess the presence of (intermediate) metal carbides during the different stages of carbon deposition. The carbide content in the early stages of filamentous growth was monitored using *in situ* magnetization measurements. Carbon contents present during steady-state filamentous growth were quantitatively determined using temperature-programmed hydrogenation (TPH). Combination with measurements of the saturation magnetization (M_s) yielded information about the chemical nature of the carbon species. The identification of ferro/ferrimagnetic phases was performed employing thermomagnetic analysis (TMA). Implications for the mechanism of filamentous growth will be given.

EXPERIMENTAL

Apparatus

Magnetic measurements were performed using a modified Weiss-extraction method (Fig. 1). Ferromagnetic samples could be magnetized in fields up to 0.52 MA m^{-1}. The magnetic field (H) was produced by a Newport Type A electromagnet with 60-mm pole faces separated by a 46-mm gap. Between the magnet poles two interrupted Helmholtz sensing coils were mounted coaxially. These pick-up coils were 20 mm in diameter and each contained 18,000 turns of insulated copper wire (diameter 0.1 mm). They were connected in series, but in an opposite sense to minimize disturbances caused by field fluctuations. Extraction of the magnetized sample from the pick-up coil generates an induction voltage. The time integral of the induction voltage corresponds to the net change of magnetic flux at the pick-up coil. Integration was done after amplification (1000×). Instead of displacing the specimen, in our modification of the Weiss-extraction method the electromagnet could be transported along two rails over any desired distance. The magnetization of samples could be measured at temperatures

ranging from 100 up to 740 K using an indirect air cooler/heater. The quartz sample holder was connected to a conventional Pyrex high-vacuum system, equipped with a quadrupole mass spectrometer (Leybold-Heraeus Q 200). The sample holder was also suited for atmospheric flow experiments allowing for simultaneous mass-spectrometric gas analysis. Temperature-programmed experiments could be carried out at heating rates ranging from 1.7 to 300 mK s^{-1}.

In some experiments also a vibrating-sample magnetometer was used. The principle of this technique has been clearly outlined in Ref. (*16*). This apparatus enables us to perform magnetization experiments at liquid-nitrogen temperature at a field strength up to 1.12 MA m^{-1}. After the catalyst pretreatment (reduction or carburization) 50 mg of the catalyst was brought into the sample holder under a nitrogen atmosphere to prevent oxidation of the sample.

Procedures and Catalysts

Thermomagnetic analysis was performed at the maximum field strength (0.52 MA m^{-1}). These analyses were carried out in a helium atmosphere or in a flow of 10 vol% of hydrogen diluted with argon at a total flow rate of 0.14 cm^3 s^{-1}. The magnetically monitored transient carburization experiments were also measured at the maximum field strength. To prevent displacement of catalytic material during the magnetic measurements the reactor bed was covered with a layer of quartz fragments. The saturation magnetization at room temperature was determined by linear extrapolation of the M versus $1/H$ plot.

Temperature-programmed hydrogenation was performed at a heating rate of 0.1 K s^{-1} using a flow of 0.8 cm^3 s^{-1} of 10 vol% hydrogen in argon. Mass-spectrometric analysis was employed, scanning eight selected m/e values within 24 s.

Preparation and pretreatment of the catalysts as well as the carburization procedures have been extensively described elsewhere (*1*). For the nickel catalyst reported on in this paper the dispersion was estimated to be 0.1 [the Langevin low-field estimate (*17*) for the mean particle size (assuming spherical particles) was 5.4 nm]. The dispersion of the iron catalyst was estimated to be 0.02 from X-ray line broadening, using the Scherrer equation.

RESULTS

Nickel Catalysts

A. Transient carburization behavior. To investigate the transient behavior of nickel catalyst particles concurrent with filamentous carbon growth, the magnetization of a freshly reduced 50 wt% Ni/SiO_2 catalyst (reduction temperature 870 K) was monitored as a function of time. As electron microscopy (*1*) revealed that nickel particles with a diameter larger than 10 nm were involved exclusively in filament growth, the measurement of the magnetization should be performed under conditions that give high weighting to the larger particles. The moderate H/T values applied guarantees that nickel atoms present in larger particles predominantly contribute to the observed magnetization. Figure 2 shows the time dependence of the magnetization during carburization with 10 vol% of methane in nitrogen at a flow rate of 0.8 cm^3 s^{-1}. The magnetization was measured during 15 ks, while also after a period of 65 ks a final measurement was made. Methane was chosen as the carburizing agent to prevent interference by Ostwald ripening of nickel particles due to transport via $Ni(CO)_4$. The magnetization was followed during carburization at three different temperatures, viz. 576, 596, and 611 K. Initially a decrease of the magnetization was observed. Having passed through a minimum, the magnetization gradually increased up to typically 70% of the original value, as shown in Fig. 2. Attention should be paid to the relative decrease of the magnetization down to about 25% in the case of carburizing with methane, whereas carburizing with CO at 540 K

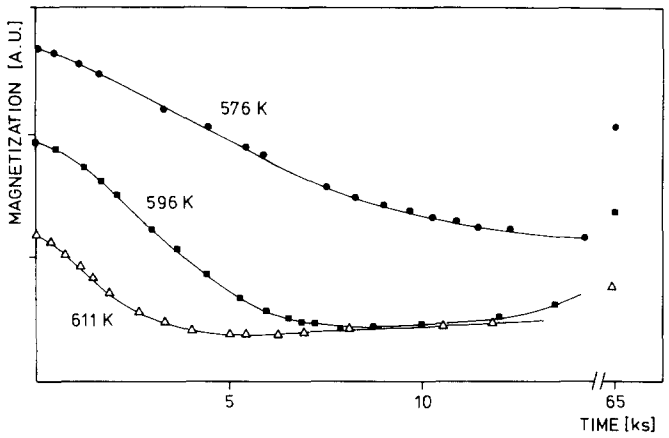

FIG. 2. Time dependence of the magnetization of a 50 wt% Ni/SiO_2 catalyst during carburization with 10 vol% CH_4/N_2. The carburization temperatures are indicated. Note the value of the magnetization realized after 65 ks.

results in a complete loss of ferromagnetic behavior (*18*). The decrease of the magnetization cannot be associated with the formation of a surface carbide only, the metal dispersion being 0.1. Also the 0.02 at.% interstitially dissolved carbon predicted from solubility data (*19*) is not expected to destroy as much as 75% of the ferromagnetism. Hence, we may conclude that a bulk carbide is formed preceding the nucleation of graphite. The question whether a stoichiometric carbide is required for the nucleation of graphite, however, cannot be answered from these experiments. The observation of the gradual increase of the magnetization indicates that after the nucleation of filamentous carbon the carbon content is significantly lower than that realized in the very early stages of carburization.

Replacing the carburizing agent by a 10 vol% H_2/Ar mixture at 576 K results in an almost instantaneous recovery of the origi-

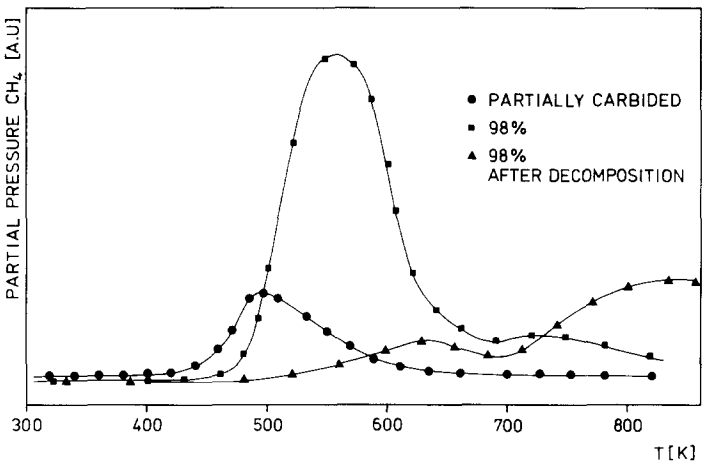

FIG. 3. Temperature-programmed hydrogenation profiles of a 50 wt% Ni/SiO_2 catalyst, after carburization with 100% CO at 540 K during 4 ks (circles); after carburization during 20 ks (squares); after carburization during 20 ks followed by decomposition at 620 K in a He atmosphere during 8 ks (triangles). The percentages refer to the relative decrease of the magnetization observed after the carburization treatment.

nal magnetization. The rate of recovery is limited by the supply of hydrogen.

To investigate the generality of the involvement of carbides in filament growth, irrespective of the nature of the carburizing agent, the transient behavior of nickel was also studied during carburization with carbon monoxide. Here temperature-programmed hydrogenation was selected to provide information on the content of carbide in the sample, as the TPH profiles are not significantly affected by changes in the particle size distribution (as was the case with the above magnetization measurements). In Fig. 3 TPH profiles of Ni/SiO_2 catalysts exposed to 100% carbon monoxide (flow rate 0.8 $cm^3\ s^{-1}$, temperature 540 K) are collected. It can be seen that a short exposure (4 ks) leads to a profile characteristic of carbidic material (*1*), whereas a longer exposure (20 ks) leads to TPH peaks of both carbidic carbon and a small amount of filamentous carbon. The transient character of the carbide phase is clearly illustrated by decomposing a 100% carburized sample (that is, a sample which has lost superparamagnetic behavior due to decoupling of all nickel atoms) during 8 ks at 620 K in a flow of inert gas. The decomposition causes the hydrogenation behavior characteristic of carbidic material to disappear in favor of that of filamentous carbon accompanied by the recovery of the original magnetization. These TPH experiments again indicate that a carbide phase is formed preceding the nucleation of filamentous carbon.

B. Steady-state carburization behavior. In order to identify the carbon present in nickel during steady-state filament growth and to determine the amount of this carbon, the following experiments were performed. Nickel catalysts were reduced at 870 K for at least 20 ks to assure a degree of reduction of 100%. The saturation magnetization of the freshly reduced catalyst was measured after flushing with nitrogen at 850 K. Subsequently, 10 vol% methane in nitrogen was fed to the reactor at temperatures ranging from 723 to 773 K, until the effluent gas composition was time-invariant, indicative of steady-state carburization. The sample was thereupon quenched to room temperature, simultaneously replacing the carburizing agent by nitrogen, and M_s was again measured. In separate desorption experiments it was verified that the observed decrease in M_s was not due to the amount of hydrogen and methane adsorbed during the quenching procedure. The amount of carbidic carbon was accurately determined using TPH with gas-chromatographic determination of methane as described in our previous paper (*1*). Hydrogenation was performed at a heating rate of 11 mK s^{-1} up to a temperature of 573 K, ensuring a complete reduction of only the carbide phase. After TPH the sample was flushed with nitrogen at 850 K and again M_s was determined. After the first hydrogenation of a carburized sample typically 95% of the original M_s was measured. All subsequent carburization–hydrogenation cycles did not result in a further loss of saturation magnetization. Attention was focused on the reversible changes in M_s. The results for five different carbon contents are collected in Fig. 4. Here the bond number, i.e., the number of nickel atoms (ferro)magnetically eliminated by one carbon atom, is plotted

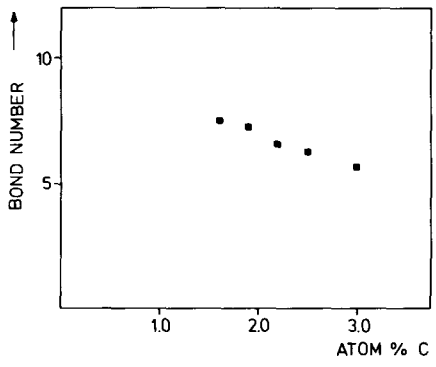

FIG. 4. Bond numbers of carbon present during steady-state filament growth as a function of the carbon content.

against the carbon content of the sample. It is seen that bond numbers decrease with increasing carbon contents. The carbon contents realized under the specified conditions yield bond numbers of 6 to 7. The carbon contents greatly exceed the reported solubility of interstitial carbon in nickel (*19*).

The above bond numbers were determined from changes in the saturation magnetization. The estimation of the values of M_s was obtained by extrapolation of M versus H/T curves, using H/T values between 1.5 and 1.7 kA m^{-1} K^{-1}. Although Richardson and Desai (*20*) demonstrated that the extrapolation procedure from measurements at comparable magnetic fields (0.64 MA m^{-1}) yielded similar results as obtained from the extrapolation from ultrahigh field measurements (up to 8.0 MA m^{-1}), it may be questioned whether the reported extrapolation procedure is correct with the catalyst used in this investigation. Therefore, we collected M versus H/T curves employing the vibrating-sample magnetometer to estimate M_s from the region 1.5–1.7 and 13–14.2 kA m^{-1} K^{-1}. For the freshly reduced sample the low-region estimate was found to be 12.5% lower than the high-region estimate. For carburized samples the underestimation amounted to 14.6%. As the vibrating-sample magnetometer did not allow for *in situ* measurements, we performed the bond number determinations at the lower H/T values in the apparatus described extensively above. The consequences of the underestimation of M_s will be discussed below.

To investigate whether the carbide present during steady-state filament growth is preferentially localized in nickel particles of a particular size range, the relative magnetization (M/M_s) versus H/T was measured for the freshly reduced catalyst as well as for the carburized catalyst. As the initial slope of the relative magnetization curve (Langevin low-field method (*17*)) after carburizing decreased by typically 10%, we conclude that the carbide present during steady-state filament growth is almost equally distributed over large and small nickel particles.

Iron Catalysts

Also in the case of iron the original aim of this study was to identify the intermediate carbide as well as to investigate the transient behavior of iron catalyst particles concurrent with filamentous carbon growth. The analysis of carburized iron samples is complicated due to the existence of at least six ferromagnetic carbides under the conditions used in our experiments: θ-Fe_3C, ε-Fe_2C, ε'-$Fe_{2.2}C$, χ-Fe_5C_2, Fe_xC, and Fe_7C_3, in the nomenclature of Niemantsverdriet *et al.* (*21*). It should be realized, however, that in the case of iron a particular carbide may not only be an intermediate in filament growth, but also an intermediate in reactions leading to more stable iron carbides. Recording the magnetization as a function of time is thus not equivalent to monitoring the amount of the carbide intermediate in filament growth, as was the case with nickel. The interpretation of changes in magnetization during the early stages of filament growth requires TMA of the sample at regular time intervals. Apart from the continuous formation of θ-Fe_3C the gradual changes in the amounts of the other ferromagnetic compounds are not believed to have sufficient significance. In this paper we therefore confine ourselves mainly to the identification of the intermediate carbide in the early stages of filament growth.

An iron/alumina catalyst was carburized in a flow of 100% carbon monoxide (0.8 cm^3 s^{-1}) at 620 K. Thermomagnetic analysis of the phases formed was performed after quenching in an inert gas flow. A 10 vol% hydrogen/argon mixture was passed over the catalyst during the thermomagnetic analysis. Figure 5 shows two thermomagnetic curves, obtained after carburizing for 1 and 6 ks, respectively. Both curves were measured at rising and declining tempera-

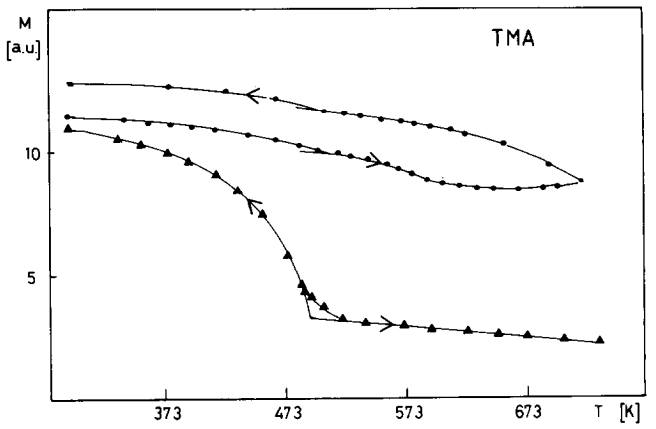

FIG. 5. Thermomagnetic analysis of a 50 wt% Fe/Al_2O_3 catalyst in a 10 vol% H_2/Ar atmosphere after carburization with 100% CO at 620 K, during 1 ks (circles) and during 6 ks (triangles).

ture. The analyses demonstrate the presence of cementite (Curie temperature, T_c = 485 ± 8 K) in considerable quantities especially after prolonged carburization, and exclude the presence of appreciable amounts of χ-Fe_5C_2 and Fe_7C_3 (T_c, respectively, 530 ± 10 and 523 ± 3 K (*22*)). After carburizing for 1 ks the TMA curve displayed an increase of the magnetization at temperatures above 570 K due to the hydrogenation of a compound of a T_c higher than 550 K. The presence of Fe_3O_4 (T_c = 853 ± 15 K) was excluded by performing an identical carburization experiment followed by TMA measured in a helium atmosphere. Also in that case an increase of the magnetization was observed, but at a higher temperature (about 700 K). So the observed increase of the magnetization can only be attributed to the decomposition of a carbide with a T_c higher than 550 K. It should be pointed out that in the catalyst carburized for 6 ks only θ-Fe_3C and α-Fe were detected. Hydrogenation for 60 ks at 740 K did not result in any recovery of the magnetization. Under these conditions θ-Fe_3C is stable against decomposition and even against hydrogenation. Hence, the only carbides responsible for the increase of the magnetization can be the hexagonal carbides ε-Fe_2C or ε'-$Fe_{2.2}C$ (T_c, respectively, 653 and 723 K). For Fe_xC no T_c has been reported, so the present analysis cannot yield information on its possible involvement.

Finally, the intermediate carbide present during steady-state filament growth was investigated. The above experiments indicated that after prolonged carburization the concentration of the intermediate carbide is rather low; we thus had to use our most sensitive detection technique (TPH) to identify the intermediate. An iron catalyst was subjected to TPH after quenching in an inert gas from a carburization experiment at 860 K. Methane was used as the carburizing agent. X-Ray analysis as well as thermomagnetic analysis demonstrated that the main carbide phase present was cementite. Figure 6 displays the TPH characteristics. From the transient experiments described above it was deduced that the only carbides present were θ-Fe_3C and ε-Fe_2C or ε'-$Fe_{2.2}C$ carbides. As hydrogenation of θ-Fe_3C does not proceed at temperatures below 740 K, the first peak (610 K), corresponding to 3.6 at.% of carbon in Fe, was tentatively attributed to the hydrogenation of ε-Fe_2C or ε'-$Fe_{2.2}C$. However, no direct evidence from magnetic measurements or from X-ray diffraction could be derived for this proposition. Whereas X-ray patterns measured after quenching from a temperature of 650 K revealed the presence

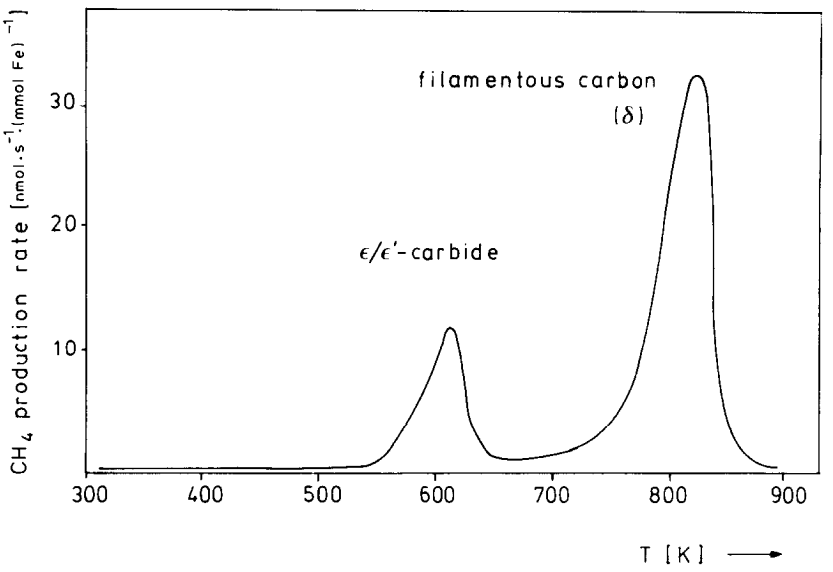

FIG. 6. Temperature-programmed hydrogenation profile of a 50 wt% Fe/Al_2O_3 catalyst after steady-state carburization with 10 vol% CH_4/N_2 at 860 K.

of θ-Fe_3C, α-Fe, and graphite, X-ray analysis performed after hydrogenation up to 900 K only indicated the presence of α-Fe. This implies that the most pronounced hydrogenation peak (800 K) corresponds to the hydrogenation of both filamentous carbon and θ-Fe_3C.

DISCUSSION

Nickel Catalysts

A great number of publications report on the formation of nickel carbide under a variety of experimental conditions (*24, 25*). Also the decomposition of nickel carbide is rather well documented (*26–28*). In this study we provided evidence that a high carbide content is a prerequisite for nucleation of graphite. A few remarks have to be made. First, the transient decrease in magnetization reported is not limited to the fraction of nickel involved in filament growth. As mentioned above, electron microscopic analysis revealed that only carbon filaments were grown with a diameter larger than 10 nm, while the Langevin low-field estimate for the mean particle size indicates a fraction of the nickel to be present in smaller particles. We cannot rule out that initially also carburization of these small particles takes place, followed by decomposition not leading to filament growth. Although the fraction of nickel present in small particles contributing to the initial decrease in magnetization is not accurately known, it can be excluded that the effect is entirely due to nickel in small particles, considering the magnitude of the Langevin low-field estimate for the mean particle size.

Let us now focus on the steady-state carburization behavior. The observation of a minimum diameter for the filaments could be explained assuming that small particles become encapsulated due to decomposition of carbides under carburizing conditions. The reported low activity of small nickel particles in the hydrogenation of carbon monoxide (*29*) can also be explained assuming encapsulation of small particles. Moreover, Kehrer and Leidheiser (*30*), studying the carburization of macroscopic nickel crystals at 823 K, observed a vehement carbon deposition at the minor faces

(high index planes). Small particles having a relatively large fraction of these planes in their surface are thus liable to rapid encapsulation.

One might imagine that the decomposition of the formed bulk carbide leads to a surface carbide and free carbon. Martin and Imelik (*31*) reporting on saturation magnetization studies established a bond number of 3 for a surface carbide. Thus, we can eliminate the exclusive formation of a surface carbide.

The high bond numbers we found were also measured by Martin and Imelik (*31*). They adsorbed a great variety of hydrocarbons a 196 K, and performed saturation magnetization measurements varying the "holding temperature," i.e., the temperature at which the catalyst was kept prior to the magnetic measurements. In these experiments the bond numbers gradually increased from holding temperatures of about 474 K onward. The effect was attributed to dissolution of carbon in the bulk of the metal. A possible rationalization of these high bond numbers was given by Martin *et al.* (*32*), but it should be emphasized that an adequate theory quantitatively describing the influence of dissolved foreign atoms on collective magnetism of 3*d* metals has not been developed as yet. The high bond numbers rule out that nickel is present partly as metallic nickel and partly as a stoichiometric carbide. We conclude that we are dealing with a substoichiometric carbide under steady-state filament growth conditions.

In the above paragraph the reported bond numbers were based on the extrapolation procedure to obtain M_s using H/T values between 1.5 and 1.7 kA m^{-1} K^{-1}. Previously, we reported that the degree of underestimation of M_s for the freshly reduced and the carburized sample was found to be 12.5 and 14.6%, respectively. Let us now consider the effect of the underestimation of M_s on the bond number determinations. Generally, incorporation of carbon atoms in nickel particles will induce an apparent change in the particle size distribution. Due to decoupling by interaction with carbon atoms the number of ferromagnetically coupled nickel atoms within a particle will decrease. Therefore, the degree of underestimation of M_s may be different for freshly reduced and carburized samples. Let us denote the fractional underestimation of M_s for the freshly reduced and carburized catalyst by a and b, respectively, while the fraction of nickel atoms being decoupled by the incorporation of carbon atoms is called c; the magnetization change determined according to the extrapolation procedure using too low values of H/T will be $(1 - a) \cdot M_s - (1 - b) \cdot M_s \cdot (1 - c) = M_s \cdot (c + (b - a) - bc)$ instead of $M_s - M_s \cdot (1 - c) = c \cdot M_s$.

From the above formulas, it is evident that bond numbers (the fraction of decoupled nickel atoms times the number of nickel atoms present in the sample and divided by the number of incorporated carbon atoms) may be both over- and underestimated, depending on the magnitude of a, b, and c. From the fractional estimates of a and b (0.125 and 0.146) and the apparent relative decrease of M_s (larger than 0.1, based on the extrapolation using too low H/T values), it may be deduced that the relative overestimation of the bond numbers does not exceed 7.5%. Thus, the conclusion based on the high value of the bond numbers, i.e., the substoichiometric character of the intermediate carbide, is not affected by the underestimation of M_s.

Finally, the low-field magnetization study of Kuijpers *et al.* (*33*) should be commented on in this context. It was concluded that carburizing of nickel catalysts with methane at temperatures up to 573 K results in the formation of a surface carbide only. It should be emphasized that formation of a bulk carbide at the mentioned experimental conditions in the static system used by these authors is prohibited by thermodynamics. Our study clearly indicates that considerable bulk carburization does take place at 576 K.

Iron Catalysts

A great deal of information on the structure of iron carbides was collected by Nagakura and Oketani (*22*) and Le Caër *et al.* (*34*). A few relevant data are summarized here. Carbon atoms are localized at octahedral positions or in trigonal prisms. The size ratio of iron and carbon atoms causes carbon to prefer a trigonal prismatic environment of iron atoms. Andersson and Hyde (*35*) have shown that twinning on $(1\bar{1}02)$ planes in hcp iron generates trigonal prisms in the twin plane, supplying thus an elegant description of the formation of the trigonal prismatic carbides θ-Fe_3C, χ-Fe_5C_2, and Fe_7C_3. In fact, this twinning operation corresponds to changing asymmetrically the dimensions of the interstices. The size of the unoccupied interstices decreases at the expense of those containing carbon, leading to an overall increase in density (*36*). These trigonal prismatic carbides are characterized by low Curie temperatures and by a remarkable stability as compared to the hexagonal carbides (ε-Fe_2C and ε'-$Fe_{2.2}C$), where carbon atoms occupy octahedral positions. The carbon arrangement and even the carbon content of these hexagonal carbides is still a matter of controversy.

Goodwin and Parravano (*37*) reported on a conversion electron Mössbauer spectroscopic study on the decarburization of iron films by hydrogen. They attributed the observed fast decarburization after carburization at 569 K to the presence of the less stable ε-carbide, whereas the θ- or χ-carbides precipitating above 573 K exhibited a drastically decreased rate of decarburization owing to their higher stability. Summarizing, we invoke the structure of the trigonal prismatic carbides to account for their thermodynamic stability, while the kinetic stability of these carbides has also been established experimentally.

Turning to our TMA experiments, it should be noted that an increase in magnetization at temperatures above 573 K might also be ascribed to decomposition of the paramagnetic FeO. However, it has been established (*38*) that already above 473 K this metastable oxide disproportionates to α-Fe and the ferrimagnetic Fe_3O_4. At a carburizing temperature of 620 K the presence of FeO is therefore very unlikely. As under our experimental conditions also no formation of Fe_3O_4 was observed, we conclude that all magnetization changes observed can be attributed to the formation and decomposition of carbides.

We now arrive at the identification of the carbide which is intermediate in the steady-state growth of filamentous carbon. In the above it has been proposed from TPH experiments that ε- and ε'-carbides, albeit at very low concentrations, are present in samples quenched from steady-state filament growth. Higher concentrations, detectable with TMA, are present during the early stages of growth. This transient behavior is very similar to the behavior of the hexagonal Ni_3C. Also cementite was formed, but this carbide proved to be stable against decomposition and even against hydrogenation at temperatures where extensive filament growth was observed. From these observations we conclude that hexagonal ε-carbides are the intermediates in filamentous growth, cementite being merely an inactive side product. This corroborates the conclusions of Baker *et al.* (*9*) that cementite does not give rise to filament formation. Sacco *et al.* (*14*) appear to have been monitoring the formation of a side product.

Initiation and Mechanism

The two major conclusions which we reached above, viz. the formation of a carbide preceding nucleation of carbon during the early stages of filamentous growth and the presence of a substoichiometric carbide under steady-state growth conditions, have some important implications for the understanding of the mechanism of filamentous carbon formation.

Let us first discuss the initiation process. It has been reported that nucleation of car-

bon associated with filamentous growth requires an induction period (*39*). From our *in situ* magnetization measurements it appears that high carbide contents are required before nucleation of carbon proceeds. Induction periods can thus be interpreted as the time needed for both the formation of a carbide phase of high carbon content and the incubation time (*40*) associated with the decomposition of this phase.

The details of the initial steps of carbide decomposition are not well known. Temperature and pressure (*41*) have been found to be important parameters. For nickel it has been suggested that graphite nucleates in the bulk of the carbide phase leading to fractionation of the metal crystallites (*42*). Also in the case of iron, Le Caër *et al.* (*34*) supposed that the relative increase of the contribution of superparamagnetic iron carbide to the Mössbauer spectrum could be explained by fragmentation of particles. For supported catalysts the metal particles seem to fragment most probably where mechanical stresses are easiest to dissipate, that is, at the metal–gas interface or near the metal–support interface. In the latter case nucleation of carbon takes place through precipitation of graphite layers near the metal–support interface, thereby lifting the particle from the support.

Such a fragmentation of nickel particles could explain the irreversible loss of saturation magnetization, typically 5%, observed after the first carburization. The extent of the permanent loss of saturation magnetization rises with increasing temperature. Even prolonged hydrogenation at 820 K did not result in a 100% recovery of the saturation magnetization. This effect could be due to a change of the nickel particle size distribution to a higher mean dispersion. In that case, the extrapolation procedure required to calculate the saturation magnetization can be biased, since the smallest particles (with a diameter less than 1.5 nm) are only slightly magnetized at the applied magnetic field strengths. As a result this highly dispersed nickel is beyond experimental observation. The temperature dependence can be appreciated by realizing that the number of metal particles involved in fragmentation increases with rising temperature, due to the increase of the nucleation rate.

Once a carbon phase has nucleated we enter the regime of steady-state growth. As has been mentioned in the Introduction, the major point of discussion here is the nature of the driving force for transport of carbon through the metal particle. The observed presence of carbides during steady-state growth seems to facilitate the comprehension of this growth mechanism.

The overall driving force responsible for the transport of the carbon atoms is now clear. The Gibbs free energy of the metal carbide is higher than that of its constituting elements. The driving force leading to transport of carbon atoms within the metal (carbide) particles is, however, more difficult to assess. Usually, the transport is attributed to an activity (or concentration) gradient of carbon in the metal phase. Baker *et al.* (*2, 8*) proposed that temperature differences are the origin of differences in activity of carbon leading to transport of carbon atoms. Rostrup-Nielsen and Trimm (*3*) assumed differences in activity to be caused by a different solubility of carbon species of a different origin. However, the above explanations take no account of the fact that when the carbon is taken up into a substoichiometric carbide, significant changes in the original metal structure are induced. A description of the migration of carbon through an unaltered fcc (Ni) or bcc (Fe) matrix in terms of activity gradients only, is therefore not appropriate. The transport of carbon atoms through the metal (carbide) particle may be explained by assuming the carbon content of the substoichiometric carbide to be highest at the metal–gas interface, and lowest at the metal–carbon interface, leading to transport in the direction of the metal–carbon interface. The substoichiometric character of the intermediate carbide facilitates the realization of such a gradient in carbon content. In the opinion of the present authors a

description of carbon transport in terms of a substoichiometric carbide is more appropriate, as it explains (i) the high carbon content encountered during steady-state growth (200 times the reported solubility of carbon), (ii) the observed high bond numbers, and (iii) high transport rates of carbon. Generally, transport rates in nonstoichiometric compounds are significantly higher than in stoichiometric compounds (*43*). The driving force for carbon transport is a gradient in the carbon content of a nonstoichiometric carbide. Reaction to a (substoichiometric) carbide involves both a modification of the metal structure and the establishment of a certain carbon concentration. To attribute the driving force, as usual, to a mere difference in activity of dissolved carbon is therefore not suitable; the standard chemical potential is also affected.

The concept proposed by Wada *et al.* (*10*), i.e., a different origin of carbon leading to a different concentration of this carbon when accommodated in a metal, can now be reformulated. The identity of the carbon source does not influence the solubility of carbon, but determines the way in which the carbon is taken up by the metal. Whereas formation of a metal carbide from graphite and metal is thermodynamically unfavorable and only a small amount of carbon can be interstitially dissolved, reaction with carbon-containing gases results in the formation of metastable, substoichiometric carbide compounds.

We have shown above that both for iron and nickel the intermediate carbide is of the hexagonal structure. Also in the case of cobalt a hexagonal carbide has been identified under growth conditions (*44*). It is tempting to assume that these carbides, characterized by a relatively low density, facilitate carbon transport, thereby explaining the high rates of filament formation.

CONCLUSIONS

From the combination of (saturation-) magnetization measurements and (quantitative) temperature-programmed hydrogenation experiments during steady-state filament growth as well as during the early stages of growth we conclude the following:

(i) Nucleation of graphite on nickel catalysts is preceded by the formation of a carbide phase with a high carbon content. In the case of iron during the early stages of growth a considerable amount of carbide intermediate can be detected.

(ii) The nickel carbide present during steady-state filament growth is substoichiometric.

(iii) The iron carbide intermediate is proposed to be ε-Fe_2C or ε'-$Fe_{2.2}C$, whereas the involvement of θ-Fe_3C can be definitively ruled out.

(iv) Carbon filaments grow by a continuous decomposition of a metastable carbide intermediate. The driving force for filament growth is a gradient in the carbon content of nonstoichiometric carbides, decreasing in the direction to the metal–carbon interface.

ACKNOWLEDGMENTS

The authors are indebted to Mr. H. M. Fortuin for preparing the iron catalysts. The investigations were supported by the VEG Gasinstituut n.v. and by the Netherlands Foundation for Chemical Research (SON) with financial aid from the Netherlands Organization for the Advancement of Pure Research (ZWO). Finally, the authors wish to express their appreciation to Dr. O. L. J. Gijzeman for his careful comment on this paper.

REFERENCES

1. de Bokx, P. K., Kock, A. J. H. M., Boellaard, E., Klop, W., and Geus, J. W., *J. Catal.* **96,** 454 (1985).
2. Baker, R. T. K., Barber, M., Harris, M., Feates, F., and Waite, R., *J. Catal.* **26,** 51 (1972).
3. Rostrup-Nielsen, J. R., and Trimm, D. L., *J. Catal.* **48,** 155 (1977).
4. Buyanov, R. A., Chesnokov, V. V., Afanes'ev, A. D., and Babenko, V. S., *Kinet. Katal.* **18,** 839 (1977).
5. Massaro, A., and Petersen, E. E., *J. Appl. Phys.* **42,** 5534 (1971).
6. Cooper, B. J., Trimm, D. L., and Wilkinson, A., *in* "Proceedings 4th London Int. Conf. Carbon Graphite 1974," p. 396. Soc. Chem. Ind., London, 1976.
7. Rostrup-Nielsen, J. R., *in* "Catalysis, Science and

Technology" (J. R. Anderson and M. Boudart, Eds.), Vol. 5, p. 77. Springer, Berlin, 1984.
8. Baker, R. T. K., and Harris, P. S., *in* "Chemistry and Physics of Carbon" (P. L. Walker, Jr. and P. A. Thrower, Eds.), Vol. 14, p. 83. Dekker, New York, 1978.
9. Baker, R. T. K., Alonzo, J. R., Dumesic, J. A., and Yates, D. J. C., *J. Catal.* **77,** 74 (1982).
10. Wada, T., Wada, H., Elliott, J. F., and Chipman, J., *Metall. Trans.* **2,** 2199 (1971).
11. Buyanov, R. A., *Kinet. Katal.* **21,** 189 (1980).
12. Buyanov, R. A., Chesnokov, V. V., and Afanas'ev, A. D., *Kinet. Katal.* **20,** 166 (1979).
13. Figueiredo, J. L., and Trimm, D. L., *J. Catal.* **40,** 150 (1975).
14. Sacco, A., Jr., Thacker, P., Chang, T. N., and Chiang, A. T. S., *J. Catal.* **85,** 224 (1984).
15. Audier, M., Bowen, W., and Jones, W., *J. Cryst. Growth* **63,** 125 (1983).
16. Zijlstra, H., *in* "Series of Monographs on Selected Topics in Solid State Physics" (E. P. Wohlfarth, Ed.), Vol. 9, p. 16. North-Holland, Amsterdam, 1967.
17. Selwood, P. W., *in* "Chemisorption and Magnetization," p. 46. Academic Press, New York, 1975.
18. Kuijpers, E. G. M., Ph.D. thesis. State University of Utrecht, Utrecht, 1982.
19. Lander, J. J., Kern, H. E., and Beach, A. L., *J. Appl. Phys.* **23,** 1305 (1952).
20. Richardson, J. T., and Desai, P., *J. Catal.* **42,** 294 (1976).
21. Niemantsverdriet, J. W., van der Kraan, A. M., van Dijk, W. L., and van der Baan, H. S., *J. Phys. Chem.* **84,** 3363 (1980).
22. Nagakura, S., and Oketani, S., *Trans. Iron Steel Inst. Jpn.* **8,** 265 (1968).
23. McCarty, J. G., Hou, P. Y., Sheridan, D., and Wise, H., *in* "Coke Formation on Metal Surfaces" (L. F. Albright and R. T. K. Baker, Eds.), ACS Symposium Series 202, p. 253. Amer. Chem. Soc., Washington, D.C., 1982.
24. Palczewska, W., "Advances in Catalysis," Vol. 24, p. 245. Academic Press, New York, 1975.
25. Kleefeld, J., and Levenson, L. L., *Thin Solid Films* **64,** 389 (1979).
26. Smith, M. A., Sinharoy, L., and Levenson, L. L., *J. Vac. Sci. Technol.* **16,** 462 (1979).
27. Sinharoy, S., and Levenson, L. L., *Thin Solid Films* **53,** 31 (1978).
28. Tøttrup, P. B., *J. Catal.* **42,** 29 (1978).
29. van Meerten, R. Z. C., Beaumont, A. H. G. M., van Nisselrooij, P. F. M. T., and Coenen, J. W. E., *Surf. Sci.* **135,** 565 (1983).
30. Kehrer, V. J., Jr., and Leidheiser, H., Jr., *J. Phys. Chem.* **58,** 550 (1954).
31. Martin, G., and Imelik, B., *Surf. Sci.* **42,** 157 (1974).
32. Martin, G., Dalmai-Imelik, G., and Imelik, B., *in* "Adsorption-Desorption Phenomena" (F. Ricca, Ed.), p. 433. Academic Press, New York, 1972.
33. Kuijpers, E. G. M., Breedijk, A. K., van der Wal, W. J. J., and Geus, J. W., *J. Catal.* **72,** 210 (1981).
34. Le Caër, G., Dubois, J. M., Pijolat, M., Perrichon, V., and Bussière, P., *J. Phys. Chem.* **86,** 4799 (1982).
35. Andersson, S., and Hyde, B. G., *J. Solid State Chem.* **9,** 92 (1974).
36. Fasiska, E. J., and Jeffrey, G. A., *Acta Crystallogr.* **19,** 463 (1965).
37. Goodwin, J. G., and Parravano, G., *J. Phys. Chem.* **82,** 1040 (1978).
38. Schieber, M. M., *in* "Series of Monographs on Selected Topics in Solid State Physics" (E. P. Wohlfarth, Ed.), Vol. 8, p. 159. North-Holland, Amsterdam, 1967.
39. Renshaw, G. D., Roscoe, C., and Walker, P. L., Jr., *J. Catal.* **18,** 164 (1970).
40. Hofer, L. J. E., Cohn, E. M., and Peebles, W. C., *J. Phys. Colloid Chem.* **54,** 1161 (1950).
41. Escoubes, M., and Eyraud, C., *Bull. Soc. Chim. Fr.,* 1374 (1966).
42. Nagakura, S., *J. Phys. Soc. Jpn.* **12,** 482 (1957).
43. Kingery, W. D., "Introduction to Ceramics," p. 236. Wiley, New York, 1967.
44. Renshaw, G. D., Roscoe, C., and Walker, P. L., Jr., *J. Catal.* **22,** 394 (1971).